Surface forces in a confined polymer melt: Self-consistent field analysis of full and restricted equilibrium cases

F. A. M. Leermakers[1] and H. J. Butt[2]
[1]*Laboratory of Physical Chemistry and Colloid Science, Wageningen University, Dreijenplein 6, 6708 HB, Wageningen, The Netherlands*
[2]*Max-Planck-Institute for Polymer Research, Ackermannweg 10, 55128 Mainz, Germany*
(Received 18 January 2005; published 18 August 2005)

In full equilibrium the self-consistent field theory for a homopolymer melt confined between two surfaces predicts pronounced oscillatory interaction forces on the monomer length scale. However, when not all the polymer molecules can reversibly equilibrate with the bulk, the trapped molecules may be squeezed, adding a repulsive contribution to the interaction energy. The classical constrained or restricted equilibrium approach by Scheutjens and Fleer two decades ago to deal with this for polymers adsorbed from dilute solutions, breaks down in semidilute and concentrated polymer solutions. We present a generalized restricted equilibrium ansatz applicable also for concentrated polymer solutions. The key idea is that only the adsorbed polymer molecules, i.e., molecules that touch the surface at least once, are forced to remain inside the gap, whereas the nonadsorbing chains are free to move out of the gap when the surfaces approach each other. As in dilute solutions, the forces found in confined melt with trapped adsorbed chains become repulsive. We analyse the dependence of the interaction forces both in full as well as in restricted equilibrium cases as a function of the chain length and the interactions with the surface for a compressible polymer melt.

DOI: 10.1103/PhysRevE.72.021807 PACS number(s): 83.80.Sg, 68.37.Ps, 67.57.Np

I. INTRODUCTION

To disperse particles in a polymer melt and make a composite material is a topic of large practical importance. To achieve good dispersion, a rule of thumb is to make sure that the polymer phase wets the surface of the particles. Being in the wetting regime ensures that the polymers spontaneously form a thick polymer film around each particle. The particles submerge in the polymer environment and avoid the polymer melt-vapor interface. For a successful incorporation of particles in the polymer melt, it is additionally necessary to have repulsive interactions between the particles.

At present there is incomplete knowledge about how a polymer melt influences the interaction between particles. Even less is known about how this interaction is related to the wettability of the polymer on the surface of the particles. This lack of knowledge is in partly due to the conflicting pieces of information provided by experiments and theory. Some information is due to surface force experiments by the surface forces apparatus (SFA) or the atomic force microscope (AFM). In addition, surface forces are analyzed by self-consistent field (SCF) theory and computer simulations.

de Gennes [1] argued that in the melt the polymers should not generate a long-range interaction force as long as chains can exchange reversibly with the bulk solution. Only when the chains are pinned at the surfaces, a repulsive interaction in the range of the radius of gyration should exist. In this pinned case the fraction of entrapped segments decreases with confining distance as a Gaussian, and as a result an exponential decrease in the repulsive force is expected. Ausserré [2] showed that (again in full equilibrium) the chain deformation exactly compensates the decreasing number of chains in the gap so that forces on the length scale of the coil size vanish. The self-consistent field theory is expected to describe the equilibrium properties of a confined polymer melt rather accurately because the mean-field approximation tends to be reliable for concentrated polymer systems. Monte Carlo computer simulations by ten Brinke *et al.* [3] showed that the chains become deformed on distances below $2R_g$, but that this indeed does not result in a long-range interaction. Dickman and Hall [4] studied dense systems of hard sphere oligomers near surfaces and observed layering effects, proving that on the monomer length scale various features must be expected.

SCF analysis of interacting surfaces in the presence of dilute and semidilute polymer solutions suggests that attraction prevails [5,6]. The qualitative aspect of the polymer-induced interaction force does not depend on the affinity of the polymers for the surface nor on the solvent quality. In dilute and semidilute solutions one considers basically two scenarios. Because of the cooperative nature of the many segments along the polymer chains, they are either strongly attracted to the surface or are depleted from it. In the adsorbed layer one may distinguish between train fragments (which are sequences of segments that are in direct contact with the surface), loops (which are sequences of segments in between the trains), and tails (which are chain fragments that are connected just to one train, leaving one end freely dangling in the solution). In the presence of two nearby surfaces it is possible that a loop transforms into a bridge; the latter is a chain fragment that is connected to two trains on opposite surfaces. The formation of bridges is entropically favorable and leads to attractive forces. The importance of tails in the adsorbed layer has extensively been discussed by Scheutjens *et al.* [7], but the repulsive effect of tails on the interaction between surfaces was put forward by Johner *et al.* [8]. This small repulsion on the length scale of the radius of gyration of the molecules was verified using numerically exact SCF modeling [9].

In the depletion case there is a region with reduced polymer density [10,11]. When two particles come in close prox-

imity, it may occur that the depletion layers overlap. The attractive force that results from this overlap may be explained from an osmotic force argument: the particles are pushed toward each other as a result of the imbalance of the osmotic force. The range of the attractive interactions is given by the radius of gyration in dilute solutions and becomes the bulk correlation length in semidilute solutions. In the limit of a melt, the bulk correlation length becomes of the monomer size and the situation may become significantly different.

On a more theoretical level the attraction in both the adsorption as well as in the depletion mode may be traced back to the fact that there is only a weak ranking number dependence; middle segments in the chain behave in first order, the same as end segments. In the SCF model one typically makes use of the Edwards equation to obtain the partition function of a single chain [13]. Although the exact results can only be reached, numerically, using the ground-state approximation, which ignores the ranking number dependences, surprisingly accurate analytical solutions become available. de Gennes showed that the ground-state eigenfunction g, which is the square root of the polymer volume fraction, $g^2=\varphi$, is a symmetric order-parameter profile in a Ginzburg-Landau free energy functional [14]. In symmetrical boundary conditions (two identical surfaces), it is straightforward to show that one should expect attractive interactions between the surfaces. One may use this argument to predict that, also in confined concentrated polymer solutions, attractive interactions should be expected. However, one should be cautious jumping too quickly to this conclusion. It is known that the ground-state approximation becomes unreliable near the adsorption-desorption transition for interfacial polymer systems. In the critical region of adsorption energies, the interaction force is nonmonotonic [11,12]. A similar failure of the ground-state approximation may occur for dense systems in which the excluded-volume effects are screened. Below we show that for a compressible polymer melt the numerically exact SCF model predicts that the forces become oscillatory.

Surfaces forces across confined polymer melts have been measured with the SFA [15–25] or the AFM [26–28]. In early SFA experiments, strongly repulsive interaction forces were always found. More recently AFM experiments show that the picture is more complex. Using SiO_2 and mica surfaces in a melt of relatively long poly(dimethylk siloxane) (PDMS) chains ($M_w=18\,000$ g/mol) revealed monotonically repulsive forces, but a melt composed of short chains ($M_w=4200$ g/mol) showed a strong repulsion only at short separation, which was proceded by a weak attraction [27].

The natural explanation for the disparity between theory and experiments is that the confined polymer melt is not in full equilibrium on the time scale of the force experiment [1]. One may argue that in the SFA, where two relatively large surfaces are broad in close proximity, it is time consuming to equilibrate the system with respect to the redistribution of macromolecules within the slit and bulk solution. Trapped molecules that are unable to diffuse out of the gap may be strongly compressed. This leads to a repulsive contribution to the interaction force. In line with this, early SFA experiments for polymers adsorbing from dilute solutions proved that the surface forces become mainly repulsive at strong confinement [29–31].

The restricted equilibrium has been implemented in the SCF theory by Scheutjens and Fleer [6]. In the restricted equilibrium case, the surfaces are first put sufficiently far apart and, for a given volume fraction of polymer in the bulk, the total amount of polymer in between the surfaces is computed. This amount is fixed during the subsequent analysis, wherein the distance between the surfaces is reduced. Thus, upon approach of the surfaces only the (monomeric) solvent can leave the gap. Using this partial open system, it was possible to reproduce the experimental SFA findings, at least qualitatively [6].

The restricted equilibrium SCF analysis as presented by Scheutjens and Fleer cannot be applied to semidilute and concentrated polymer solutions. It is obvious that by restricting all the macromolecules to remain inside the gap, one will not only squeeze the interfacial molecules, but also the many nonadsorbed, trapped chains, into a smaller volume. It is expected, however, that the nonadsorbed chains are more mobile than the adsorbed ones. The expected separation of time scales for translational mobility suggests a generalized restricted equilibrium ansatz. Below we show that it is possible to compute the number of adsorbed chains (i.e., chains that touch the surface at least once), as well as the amount of nonadsorbing chains. Following the classical work of Scheutjens and Fleer we compute the number of adsorbed chains per unit area for the case when the two surfaces are well apart. Then, upon decreasing the surface separation, we constrain the number of adsorbed chains to remain constant, whereas the amount of free chains can adjust, i.e., can exchange with the bulk. When the two surfaces get closer, nonadsorbed polymer may be removed from the gap. Only when the surfaces are at a distance of order of the radius of gyration R_g does one start to squeeze the restricted molecules, similar as in the case of the dilute solutions. In line with the arguments of de Gennes [1], we show that within this approach the interaction free energy may become repulsive rather than attractive.

In this paper we first introduce the SCF theory using the discretization scheme of Scheutjens and Fleer and focus, in particular, on the evaluation of adsorbed and free chains. In the results section we first consider the polymer-vapor interface, then shift the attention to a compressible melt next to a single solid boundary, and finally focus on the interaction between two surfaces in a compressible polymer melt. The findings are summarized at the end of the paper.

II. SCHEUTJENS-FLEER SELF-CONSISTENT FIELD THEORY

The SCF theory of polymer solutions exclusively relies on the Edwards equation to obtain the single-chain partition function [13]. This Edwards equation is a convenient starting point for further analytical analysis. The analytical analysis typically makes use of the so-called ground-state approximation. The accuracy can be established *a postiori* by comparing results to numerically exact SCF results. Here we are interested in the exact (SCF) analysis, which solves the gov-

erning equations numerically. Solving differential equations on a computer involves a discretization scheme. We will follow the approach of Scheutjens and Fleer [33,34] and Fleer *et al.* [35], who suggested introducing just one length scale l. Using this length we define the size of a lattice site as well as the segment size of the polymer. We are interested in a polymer melt composed of monodisperse homopolymers (composed of united segments, which we refer to with the segment type P) with segment ranking number $s=1,\ldots,N$, where N is the degree of polymerization. This polymer melt resides on a discrete coordinate system with lattice layers at $z=1,\ldots,H$. On both sides of the system, a flat impenetrable solid wall is present. This means that there are absorbing boundary conditions both at $z=0$ as well as at $z=H+1$. The impenetrable surfaces are composed of homogeneous material denoted with S; this means that there is a permanent volume fraction profile $\varphi_S(0)=\varphi_S(H+1)=1$ and $\varphi_S(z)=0\,\forall\, z\in\{1,H\}$. The polymers in this slit with width Hl are in equilibrium with an unconstrained melt. Here and below we will normalize all length by the segment length l, i.e., the distance between the surfaces is given by the dimensionless distance H rather than the distance Hl.

We are interested in a compressible melt, which implies that we allow for vacancies in between the polymer chains, i.e., we use a lattice-gas approach. It is known that the lattice gas exactly maps on an incompressible binary system, featuring a polymer in a monomeric solvent V. This means that the vacancies play the role of a poor solvent. In this incompressible system we consider short-range nearest-neighbor exchange interactions $\chi\equiv Z/(2k_BT)(2U_{PV}-U_{PP}-U_{VV})$ of the Flory-Huggins type between polymer and "solvent" segments [32], where Z is the lattice coordination number and U is the interaction energy. The polymer-vapor system is strongly segregated, that is the solvent is poor $\chi=-Z/(2k_BT)U_{PP}>0.5$ (here we used the fact that interactions with free volume are absent, i.e., $U_{VV}=U_{PV}=0$). A melt in equilibrium with its vapor has a well-defined volume fraction of polymer φ_b (binodal value) for value of χ. The higher the χ, the closer φ_b approaches unity. Unfortunately, there is no analytical solution of the binodal, but accurate numerical evaluations are possible.

The free volume component V not only exist in the reference bulk, but it is also in equilibrium with the free volume site within the slit. More specifically, the free volume can accumulate near the boundary, suppressing the surface density of polymers (partial wetting), or the free volume is depleted from the boundary, and the polymer density is locally high (complete wetting) [36]. The control parameter of the wetting behavior is χ_S, which is the difference of interactions between a polymer unit and a vacancy near the surface: $\chi_S=\chi_{PS}-\chi_{VS}$. Here, χ_{PS} and χ_{VS} are the Flory-Huggins parameters for the polymer-surface and vacancy-surface interactions, respectively. There exists a wetting transition at χ_S^{wet}, which is a function of the chain length N and the χ value: $\chi_S^{\mathrm{wet}}(\chi_S,N)$. Again, there are no analytical solutions for this wetting surface. Below we will pay some attention to this wetting transition.

It is of considerable interest to relate the free energy of interaction of a compressible polymer melt confined between two flat surfaces to the adsorption parameter χ_S, the chain length N, and the solvent strength χ. This means that we need to solve for the relevant partition function of the confined melt. In other words, we need to solve the appropriate SCF equations (see Ref. [35] for more details). The most unambiguous case is the so-called full equilibrium case. In full equilibrium both the polymeric as well as the vacancy component is free to equilibrate with the melt reference phase. The grand potential is the characteristic function, which can be written as $\Omega(H)=k_BT\Sigma_{z=1}^{H}\omega(z)$, where ω is the dimensionless grand potential density, k_B is Boltzmann's constant, and T the temperature. In turn, it can be written as the difference between the dimensionless bulk pressure π_b and the local dimensionless pressure $\pi(z)$, $\omega(z)=\pi_b-\pi(z)$, where

$$-\pi(z)=\ln(1-\varphi(z))+\left(1-\frac{1}{N}\right)\varphi(z)+\varphi(z)\chi\langle\varphi(z)\rangle, \quad (1)$$

and π_b is found by substituting all the local volume fraction $\varphi(z)$ by their bulk value φ_b. In Eq. (1) and below, the angular brackets indicate a three-layer average also known as the site fraction. Here, we define it as $\langle\varphi(z)\rangle=\Sigma_{z'=z-1,z,z+1}=\varphi(z')/3$. In this approach the lattice site is anisotropic: it is of size l in the z direction and $\sqrt{2}l$ in x and y directions perpendicular to z, i.e., parallel to the surface. The free energy of interaction is given by the difference between the grand potential at plate separation H and infinite separation

$$F^{\mathrm{int}}(H)=\Omega(H)-\Omega(\infty). \quad (2)$$

One characteristic of the equilibrium volume fraction profile $\varphi(z)$ is that it optimizes the grand potential Ω. It can be shown that this optimal volume fraction profiles both follows from the so-called self-consistent potentials $u(z)$ and determines this profile. In short, the segment potentials $u(z)$ are given by

$$\frac{u(z)}{k_BT}=\ln\frac{1-\varphi_b}{1-\varphi(z)}-2\chi(\langle\varphi(z)\rangle-\varphi_b)+\chi_S\langle\varphi_S(z)\rangle, \quad (3)$$

where k_BT is the thermal energy. In Eq. (3) we have used that the system is incompressible, i.e., $\varphi(z)+\varphi_V(z)=1\,\forall\, z$.

The volume fractions are found by the composition law

$$\varphi(z)=C\sum_{s=1}^{N}\frac{G(z,s|1)G(z,s|N)}{G(z,s)}. \quad (4)$$

For homopolymers, the free segment distribution function $G(z,s)$ is ranking number independent [i.e., $G(z)$] and is a Boltzmann term, which features the segment potentials [i.e., $G(z)=\exp-u(z)/k_BT$]. In the nominator of Eq. (4), there are two end-point distribution functions, which, for symmetry reasons, are mutually related [i.e., $G(z,s|N)=G(z,N-s+1|1)$]. The end-point distribution function $G(z,s|1)$ contains the combined statistical weight of all possible walks that start with segment $s'=1$ and ends with segment $s'=s$ exactly at coordinate $z'=z$, where overall starting coordinates are summed. These end-point distribution functions can be generated using a simple propagator formula

$$G(z, s|1) = G(z)\langle G(z, s-1|1)\rangle, \tag{5}$$

which is initiated with $G(z,1|1)=G(z)$.

The normalization constant in the composition law (4) is, in the case of full equilibrium, given by $C=\varphi_b/N$.

The set of Eqs. (3)–(5) is closed and solved numerically up to high precision. It is understood that the volume fraction of polymer φ_b is directly coupled to χ and follows from the Flory-Huggins theory. Alternatively, φ_b may be evaluated using Eqs. (3)–(5) for a slightly modified system in the following way. For sufficiently large values of H, one chooses one surface (e.g., at $z=1$) to have an affinity for the polymer-rich phase, and the other surface (e.g., $z=H+1$) to have an affinity for the V-rich phase. Subsequently, the system is filled only partially by polymer by choosing the normalization constant $C=\theta/[NG(N|1)]$, where the input value $\theta=\Sigma_z\varphi(z)$ is the total amount of polymer in the system (in equivalent monolayers) and $G(N|1)=\Sigma_z G(z,N|1)$ is the single-chain partition function. When, e.g., $\theta\approx H/2$, one will find a polymer-vapor interface somewhere halfway in between the gap between the two surfaces. Integrating the grand potential density [c.f. Eq. (1)] around this interface will lead to the surface tension of the polymer-vapor interface. Apart from small density variations near the two surfaces, the two bulk phases will have the correct binodal values.

III. GENERALIZED RESTRICTED EQUILIBRIUM

Let us return to the polymer melt between two identical surfaces and assume that the surfaces are very far apart. In this case the two surfaces do not interact. We need to compute the number of adsorbed molecules per unit area Γ on the surface at $z=0$ or at $z=H+1$, i.e., chains that touch the surface(s) at least once. In dilute solutions one may estimate this by the interfacial excess, i.e., $\Gamma\approx\Theta^{ex}=\Sigma_z[\varphi(z)-\varphi_b]$. However, in the limit of the polymer melt, $\Theta^{ex}\to 0$ because the bulk volume fraction approaches unity, whereas the number of adsorbed chains remains an increasing function of the polymer concentration. By definition, $\Gamma=\Sigma_z\varphi^a(z)$, where $\varphi^a(z)$ is the profile of all adsorbed chains. We will refer to the profile of polymer units that do not touch one of the surfaces $\varphi^f(z)$, as the free profile. Conservation of mass dictates that $\varphi^f(z)+\varphi^a(z)=\varphi(z)$. It turns out that it is easier to evaluate the free profile [33,34]. To do this we define a free segment distribution function with zero probability in layer $z=1$ and in $z=H$ as $G^f(z)=G(z)[1-\delta(z,1)][1-\delta(z,H)]$, which is used both as the initiator of the propagator equation $G^f(z,1|1)=G^f(z)$, in the so-called free-chain propagator

$$G^f(z, s|1) = G^f(z)\langle G^f(z, s-1|1)\rangle \tag{6}$$

and the free-chain composition law

$$\varphi^f(z) = C\sum_{s=1}^{N}\frac{G^f(z, s|1)G^f(z, N-s+1|1)}{G(z)}, \tag{7}$$

where the normalization constant remains $C=\varphi_b/N$. In Eq. (7) we divide by $G(z)$ rather than $G^f(z)$ to avoid division by zero. As the overall profile $\varphi(z)$ is known, $\Gamma=\Sigma_z[\varphi(z)-\varphi^f(z)]$ in high accuracy. It is known that in $\Gamma\propto\sqrt{N}$ in a polymer melt [37]. Besides the N dependence one should expect that χ and χ_S also affect Γ.

Below our interest will be on the free energy of interaction between two surfaces with a polymer melt in between, under the constraint that the number of adsorbed molecules both on the surface at $z=1$ and at $z=H+1$ remain constant. We will do this by introducing two polymer entities, $i=1,2$ with corresponding volume fraction profiles

$$\varphi_1(z) = \varphi^f(z), \tag{8}$$

representing the free chains, and

$$\varphi_2(z) = C_2\varphi^a(z) = \frac{\Gamma\varphi^a(z)}{\sum_z\varphi^a(z)}, \tag{9}$$

representing the renormalized adsorbed chains. Equation (9) defines the normalization constant C_2 needed to keep the total amount of adsorbed chains constant [38]. Note that when $C_2=1$, no renormalization occurred and the adsorbed chains remain in full equilibrium with the free ones. This will typically be the case when distance between the surfaces exceeds the coil size by a large amount, i.e., $H\gg 2R_g$. Of course when the adsorbed chains are confined, i.e., when $H<R_g$, we expect a larger value of the normalization constant, $C_2>1$. Now the overall volume fraction of polymer is recomputed by $\varphi(z)=\varphi_1(z)+\varphi_2(z)$.

In a system in which not all molecules are free to exchange with a reservoir, the grand potential Ω is no longer the characteristic function of this system. Instead there is a free energy of the partial open system $F^{po}(H)$ conveniently defined as

$$F^{po}(H) = \Omega(H) + \frac{\Gamma}{N}\ln C_2(H), \tag{10}$$

where Γ/N is the number of chains per unit area confined in the slit and $\ln C_2$ is the chemical potential increment of the adsorbed chains as compared to the free ones.

As in the full equilibrium case [c.f. Eq. (2)], the free energy of interaction is given by

$$F^{\text{int}}(H) = F^{po}(H) - F^{po}(\infty). \tag{11}$$

IV. RESULTS AND DISCUSSION

The results section is divided into three subsections. In Sec. IV A, we will pay attention to the polymer melt-vapor interface and consider the interfacial tension as well as the total volume fraction of polymer in the melt as a function of the governing parameters χ and N. In Sec. IV B, we compute the adsorbed amount as a function of the molecular weight and analyze the effects of χ and χ_S. We also present results $\chi_S^{\text{wet}}(\chi,N)$. In Sec. IV C, the focus is on the interaction curves, both in full as well as in restricted equilibrium. We conclude in Sec. IV D, by a case study in which we introduce a relaxation parameter to enforce only a fraction of adsorbed chains to be restricted, whereas the remaining ones are considered to be mobile. Using the restricted amount as

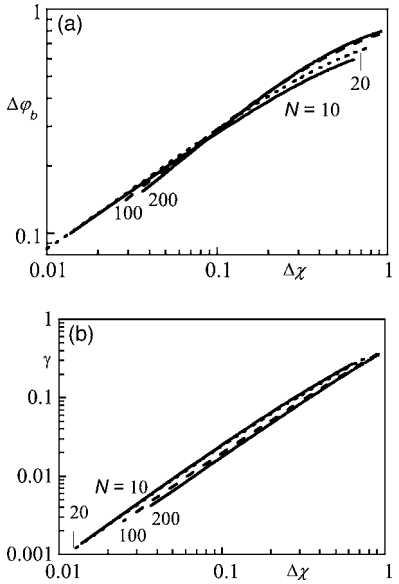

FIG. 1. (a) The difference of the polymer volume fraction of the melt and that at the critical conditions, $\Delta\varphi_b \equiv \varphi_b - \varphi_b^{cr}$ as a function of the difference between the FH parameter between polymer vapor χ and that at critical conditions $\Delta\chi \equiv \chi - \chi^{cr}$. (b) The interfacial tension γ in units $k_BT/(2l^2)$ as a function of $\Delta\chi$. The chain lengths $N=10$, 20, 100, and 200 are indicated. Note that both φ_b^{cr} and χ^{cr} depend on N.

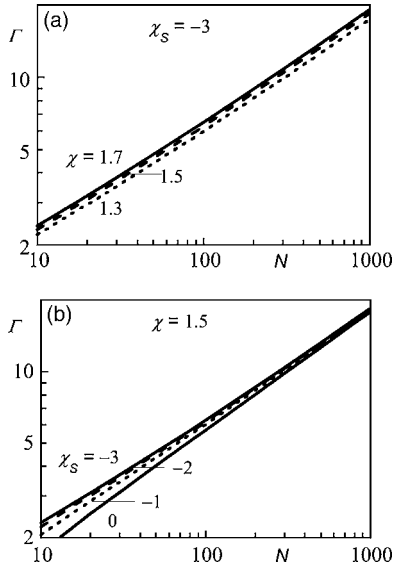

FIG. 2. The amount adsorbed onto one surface Γ in equivalent monolayers as a function of the degree of polymerization N: (a) at fixed adsorption energy $\chi_S=-3$ and for three values of χ as indicated, and (b) at fixed $\chi=1.5$ and four χ_S as indicated.

an adjustable parameter, it is possible to switch smoothly from the free to the restricted equilibrium cases.

A. Volume fraction of polymer in the melt and polymer-vapor interface

Above we argued that the compressible polymer melt in a lattice model is equivalent to a polymer in a poor monomeric solvent. For the following analysis it is necessary to know the relevant phase behavior. We therefore consider a polymer-rich phase in equilibrium with a solvent-rich phase. More specifically, a concentrated polymer phase, which is diluted in monomeric solvent, becomes in equilibrium with a concentrated monomeric-solvent phase, which is (extremely) dilute in polymers. The phase diagram of this system is the classical result of Flory-Huggins theory for which the critical volume fraction is $\varphi^{cr}=1/(1+\sqrt{N})$ and the critical Flory-Huggins parameter is $\chi^{cr}=\frac{1}{2}(1+1/\sqrt{N})^2$. It is convenient to define $\Delta\chi \equiv \chi - \chi^{cr}$ and $\Delta\varphi_b \equiv \varphi_b - \varphi_b^{cr}$. In a mean-field approximation [39] it is known that, for small values of $\Delta\chi$, the value of $\Delta\varphi_b$ vanishes as a power law, i.e., $\Delta\varphi_b \propto (\Delta\chi)^{0.5}$. This dependence is recovered rather accurately [Fig. 1(a)]. Similarly, it is known that in mean-field approximation, the interfacial tension vanishes as $\gamma \propto (\Delta\chi)^{1.5}$ for sufficiently small values of $\Delta\chi$. Also, this limiting behavior is verified [Fig. 1(b)]. Only for high values of $\Delta\chi$ and short chains, i.e., when $\Delta\chi N \gg 1$, an expected discrepancy is observed.

In the present paper, however, our interest is not in critical polymer melts because, in practice, a polymer melt is always in the strong segregation limit, i.e., for $\Delta\chi \approx 1$. From Fig. 1(a) we see that the volume fraction of polymer remains significantly below unity for all $\Delta\chi$ values used (in Fig. 1 this parameter runs up to $\chi=1.5$ for all values of N). Of course it is possible to further increase χ, and this will lead to further reduction of the free volume in the polymer melt. The truly incompressible melt is only expected for very high values of $\chi \gg 1$. For computational reasons, we will restrict ourselves to modest values of χ. From Fig. 1(a) we can extract $\varphi_b(\chi)$ accurately. Below we will use this dependence in the evaluation of the polymer melt in the presence of the surfaces as the reference concentration with which the polymers in the slit are in equilibrium. The dimensionless interfacial tension becomes of order χ in the strong segregation limit. This interfacial tension may be used to compute the contact angle of a droplet of the melt on the the surface.

B. Adsorbed amount

In this section we discuss the adsorbed amount, which is the total number of chains per unit area of which at least one segment of the chain is in touch with the solid substrate, as well as the wetting behavior of the melt on the surface. When a polymer melt is placed next to a surface, many chains will touch the surface at least once. The longer the chains, the larger is the adsorbed amount Γ. In Fig. 2 we present this adsorbed amount as a function of the chain length. In first order, one finds that $\Gamma \propto N^{0.5}$, especially for large values of N. This result has been known already for a long time [35,37]. Neither the polymer-vapor interaction parameter [Fig. 2(a)] nor the adsorption energy [Fig. 2(b)] has a strong influence on the adsorbed amount. Only for very small N is it possible to increase the adsorbed amount by increasing the surfaces affinity, i.e., by reducing χ_S. Please note that in Fig. 2 the adsorbed amount is for a single surface. In Sec. IV D when we discuss the restricted equilibrium, we restrict the same

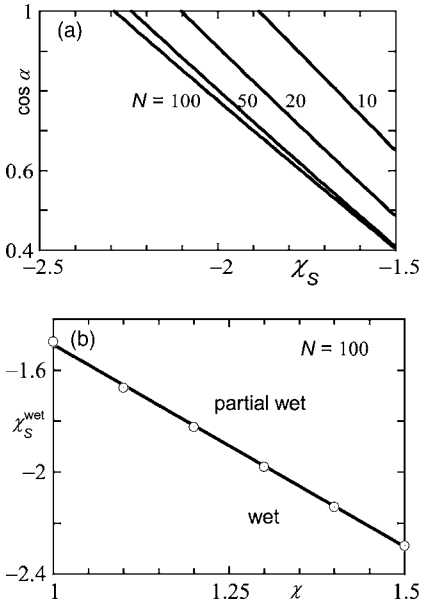

FIG. 3. (a) The cosine of the contact angle as a function of the adsorption energy χ_S for $\chi=1.5$ and four values of the chain length N as indicated. (b) The adsorption energy at the (first-order) wetting transition χ_S^{wet} as a function of the interaction energy χ for $N=100$.

adsorbed amount to each of the two surfaces. This means that the total adsorbed amount is twice that given in Fig. 2.

C. Adsorbed amount

From the introduction it is obvious that the wetting behavior is of interest for dispersing particles in a melt. More specifically, complete wetting prevents particles from adsorbing onto the polymer melt-vapor interface. We use Young's law to compute, in the case of partial wetting, the contact angle of a polymer drop sitting on a solid substrate in a vapor

$$\cos\alpha = \frac{\gamma_{SV}-\gamma_{SP}}{\gamma_{PV}} = \frac{\Omega_{\text{thin}}-\Omega_{\text{thick}}}{\gamma_{PV}} + 1. \qquad (12)$$

In Eq. (12) α is the contact angle and S, P, and V refer to the solid, polymer melt, and vapor, respectively. In Fig. 1(b) the interfacial tension of the melt-vapor interface is already given. The grand potentials $\Omega_{\text{thin}}=\gamma_{SV}$ and $\Omega_{\text{thick}}=\gamma_{SP}+\gamma_{PV}$ are computed from two adsorbed layers that are possible at the chemical potential corresponding to the bulk binodal [40]. One of them is a very thin adsorbed layer. The other one is macroscopically thick, meaning sufficiently thick such that the SP interface does not interact with the PV interface. In this limit Ω_{thick} does not depend on the actual thickness of this adsorbed film. In Fig. 3(a) we show a typical result of such an analysis. In this figure we have presented the cosine of the contact angle as a function of the adsorption energy of the polymer chains for the surface. The wetting transition χ_S^{wet} occurs when $\cos\alpha=1$. For $-\chi_S > -\chi_S^{\text{wet}}$ the polymer wets the surface. From Fig. 3(a) we see that the wetting transition shifts to more negative χ_S, the larger the chain length is. This chain length dependence is particularly noticeable for relatively small values of N. In Fig. 3(b) we have collected the adsorption energy at the wetting transition for a fixed chain length $N=100$, as a function of the polymer-vapor interaction parameter χ. The lower the χ parameter, the lower the interfacial tension γ_{PV} and the less strong the surface affinity of the polymer needs to be to have complete wetting. In the range of χ values used, χ_S^{wet} is linear in χ.

D. Force curves in full and restricted equilibrium

In this section we discuss the free energy of interaction between two surfaces that are brought into contact. It must be understood that we are only presenting the contribution of the melt and do not include the van der Waals forces or any other possible contribution. We expect that the total interaction energy is close to the sum of the polymeric and the van der Waals contribution.

From a theoretical perspective the most straightforward analysis of the free energy of interaction is the full equilibrium case. Again, in this case the polymers are in constant equilibrium with a polymer melt at fixed composition. In other words the surfaces engage sufficiently slowly so that the chemical potentials of all the interfacial chains remain exactly equal to those in the bulk. In order to relax the chemical potentials toward equilibrium, the amount of polymer in between the surface is a function of the distance between the surfaces.

In Fig. 4(a) a typical result of the interaction energy versus distance in full equilibrium for a polymer melt is shown. This interaction curve oscillates around zero. For $H=1$ the free energy of interaction is positive. For $H=2$ it is negative, for $H=3$ it is positive again, etc. The absolute value of the interaction decays exponentially (with a decay length of $\xi \approx 0.7$ in lattice units l). In the polymer melt limit, the bulk correlation length is of order unity and it is of no surprise that the features of the interaction curve occur on the length scale l. It is of interest to mention that the first minimum, which occurs at $H=2$, is sufficiently deep so that it is expected to be detectable. The secondary maximum and minimum, however, may already be more difficult to be picked up. Such oscillations have been observed with the SFA [15,25] and the AFM [26] for PDMS and tend to dramatically reduce the second virial coefficient (between particles). A sufficiently deep primary minimum has the important practical implication that it will cause the particles to assemble in clusters.

The remaining view graphs of Fig. 4 illustrate the dependences of the interaction curves on the chain length [Fig. 4(b)], the adsorption energy [Fig. 4(c)], and the polymer-vapor interaction parameter [Fig. 4(d)]. The first general conclusion of these graphs is that the interaction curves hardly depend on these quantities. As expected for the polymer melt, there is very little influence on the chain length. Only when the chain length is made sufficiently small one may observe a minor reduction of the primary maximum, accompanied by a slightly less deep primary minimum. The influence of the adsorption energy is somewhat more complicated. The value of the primary minimum goes through a

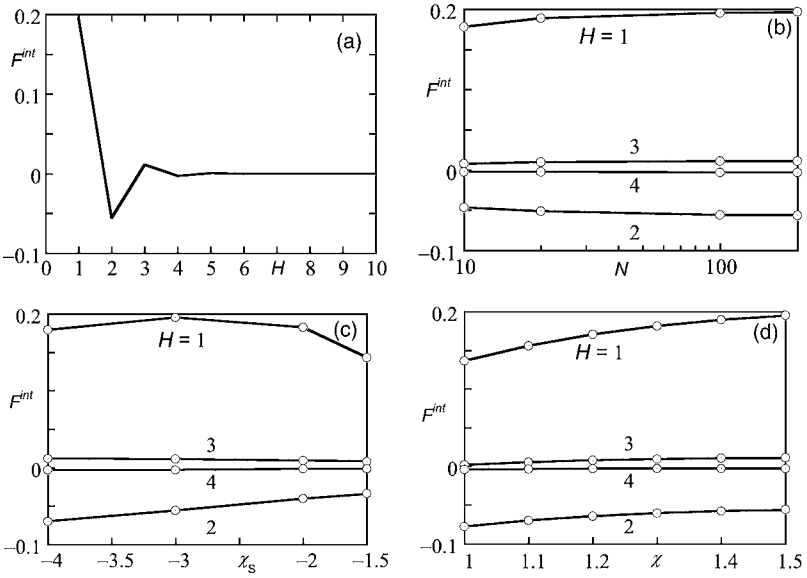

FIG. 4. Confined polymer melt in full equilibrium. (a) Free energy of interaction in units of $k_BT/2l^2$ as a function of the separation H in units l between the surfaces in the case of full equilibrium for $N=100$, $\chi_S=-3$, and $\chi=1.5$. The free energy per unit area is equal to the force divided by the radius of curvature reported in experiments. For PDMS a reasonable choice for the length scale is $l=0.8$ nm. Then the x axis goes from 0 to 8 nm and the y axis runs from -0.32×10^{-3} to 0.64×10^{-3} N/m at 25 °C. (b–d) The free energy of interaction at different separations ($H=1,2,3,4$) as a function of (b) the chain length ($\chi=1.5$ and $\chi_S=-3$), (c) the polymer-surface interaction parameter χ_S (for $N=100$ and $\chi=1.5$), and the polymer-vacancy interaction parameter χ (for $N=100$ and $\chi_S=-3$).

small maximum around the wetting value. Perhaps more significantly the primary minimum increases in depth upon increasing the affinity of the polymer for the surface. Finally, the amplitude of the oscillatory behavior tends to increase when the overall polymer density is increased, i.e., with increasing χ.

In the full equilibrium situation, relatively weak interaction forces ($F/R\leqslant 1$ mN/m) are predicted that do not much depend on the chain length. Experiments, however, showed significantly stronger forces (of the order of $F/R\leqslant 10$ mN/m at a distance of 1 nm), which significantly depend on the chain length. It is clear that in the full equilibrium case the free energy of interaction is quite generic. The wavelength of the oscillation depends strongly on the discretization level and, as such, must be considered to be only qualitatively correct. Another conclusion is that from the full equilibrium analysis one cannot explain significant and qualitative differences in the interaction curves as found by surface force experiments. For this reason it is necessary to consider the restricted equilibrium situation. Note that the restricted equilibrium as suggested here is one of the possible, and in our opinion one of the most relevant, ways in which restrictions can be implemented. Here we choose to restrict the adsorbed molecules to remain on the surface.

All view graphs of Fig. 5 represent the interaction energy for the restricted equilibrium situation of a fixed value of the adsorption energy ($\chi_S=-3$) and a fixed value of the polymer-vapor interaction parameter ($\chi=1.5$). In this figure we give the resulting free energy of interaction for various values of the length of the polymer chains. As the adsorbed amount increases with increasing chain length ($\Gamma\propto\sqrt{N}$), it is clear that the interaction curves of Fig. 5(a) diverge when $H<\Gamma$ increases with increasing N. One can easily see from Fig. 5(a) that the interactions become very strongly repulsive when the chains are strongly confined. To correct for the fact that the restricted molecules prevent the surfaces to come to full contact, we introduce the distance between the surfaces normalized to the smallest possible distance between the two surfaces, i.e., $H'\equiv H-\Gamma$. Recall that the distance is made dimensionless by the segment length and that the adsorbed

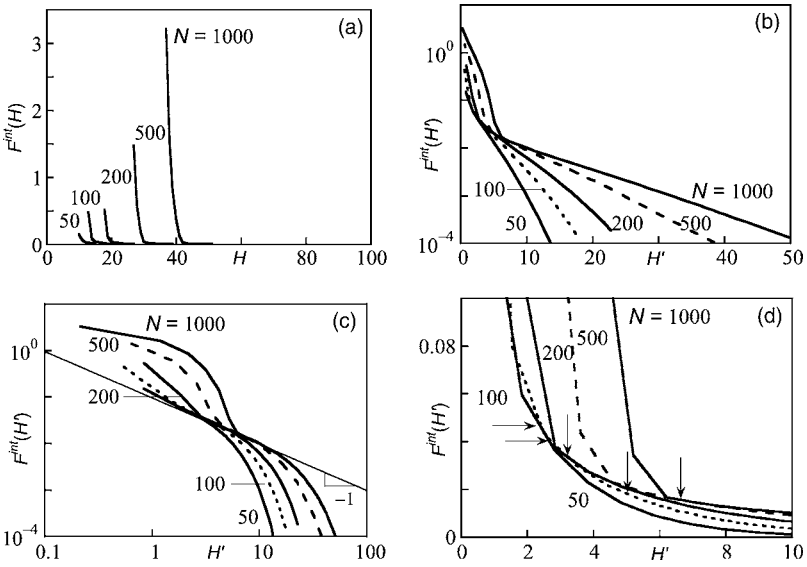

FIG. 5. Confined polymer melt in restricted equilibrium. (a) Free energy of interaction in units of $k_BT/2l^2$ as a function of the separation H in units l between the surfaces for various values of N as indicated and $\chi_S=-3$ and $\chi=1.5$. (b) The free energy of interaction in units of $k_BT/2l^2$ as a function of the scaled separation $H'\equiv H-\Gamma$ in double logarithmic coordinates. The thin line with slope −1 is discussed in the text. (c) As in (b) in semilogarithmic coordinates, (d) As in (b) in lin-lin coordinates. The arrows point to the distance H' below which no free polymer remains in the slit. Above this distance the amount of free polymer is linear in H'.

amount Γ is expressed in equivalent lattice layers; as a result both H and Γ have the same units. In the remaining graphs of Fig. 5 we use this normalized distance H'.

In Fig. 5(b) we present the force curves in semilogarithmic coordinates. From this it is obvious that all interaction curves have two exponential parts with a very distinct break (H'^*, F^*). For sufficiently high $H' > H'^*$, we see an exponential force distance relation ranging at least to $H=2R_g = 2\sqrt{N/6}$. The surfaces repel each other because the adsorbed chains on the surfaces interact. For these relatively large values of H', there are still many free chains inside the gap. Inspection shows that the overall polymer density remains roughly constant and almost equal to the polymer density of the unconfined melt. This means that when the surfaces are broad toward each other, free polymers are pushed toward the bulk. The decay length ξ of the force $F \sim \exp(-H'/\xi)$ curve is proportional to the radius of gyration, i.e., $\xi \propto R_g$. Such an exponential force-distance relation is expected for chains for which all excluded-volume correlations are screened. In other words, such force law is found when in the ground-state approximation the self-consistent potential is set equal to zero.

For very small values of $H' < H'^*$, the free chains are no longer present. In this limit the reduction of the spacing H' is only possible because the free volume V is reduced. In other words, the polymer density goes up because of the confinement. In fact, the short-range part of the interaction curve gives information on the compressibility of the polymer melt: removing all available free volume is very costly and again an exponentially force distance behavior is found. The decay length of this part of the force curve appears almost independent of the chain length N.

Interestingly, the transition region from compressing the adsorbed polymer layer by removing free volume to removing free polymer, shifts to larger values of H' and smaller values of the interaction free energy with increasing degree of polymerization N. This can be illustrated best in a double-logarithmic plot [Fig. 5(c)]. The force at this transition F^* drops inversely with the transition distance $(H')^*$, i.e., $F^* \propto 1/(H')^*$, as is shown by the thin line. Finally, in Fig. 5(d) we show an enlarged part of the interaction curve for small values of H'. In this view graph the arrows point to the distance H'^*. In surface force experiments, one should be able to see interaction free energies of order $0.05\ k_BT/2l^2$. We expect, therefore, that in such an experiment one should be able to distinguish between these two compression modes. Plotting the force curves in double logarithmic coordinates also demonstrates that there is no power-law regime.

As in the equilibrium case, it is of considerable interest to know how the curves for the free energy of interaction depend on χ and χ_S. In Fig. 6(a) we show that the adsorption energy does not change the picture significantly. This is not so surprising because we have shown that the adsorbed amount was rather insensitive to the adsorption energy. As the number of interfacial chains does not change, one cannot expect differences in the force curves. The similar conclusion can be drawn regarding the influence of the interaction between polymer and vapor χ [c.f. Fig. 6(b)]. However, the characteristic length of the exponentially increasing force at strong confinement $H < H'^*$ tends to be a decreasing function of χ. In other words, a small compressibility of the melt leads to a strong repulsion and vice versa.

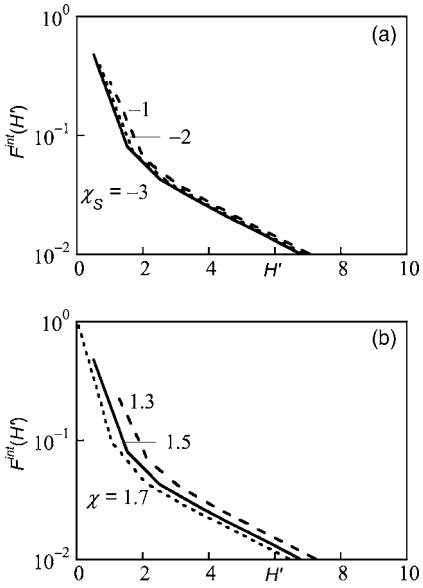

FIG. 6. Free energy of interaction in units of $k_BT/2l^2$ as a function of the separation H' in units l between the surfaces in semilogarithmic coordinates in the case of restricted equilibrium for $N=100$. (a) For various values of the adsorption energy as indicated and $\chi=1.5$. (b) For various values of the interaction energy and $\chi_S=-3$.

In Fig. 7 we show the resulting interaction curves for a case study in which we restrict a subsaturated value for the adsorbed amount of polymers to the surfaces (an equal amount to each of the two surfaces). In this system the chain length $N=100$, the adsorption energy is $\chi_S=-3$ and the interaction parameter $\chi=1.5$. From the full equilibrium case, i.e., when no chains are restricted, we know the interaction curves to be oscillatory. On the other hand, when all the molecules that touch the surface are restricted, the interaction curves are fully repulsive. One should be able to see a crossover from the full equilibrium to the restricted equilibrium

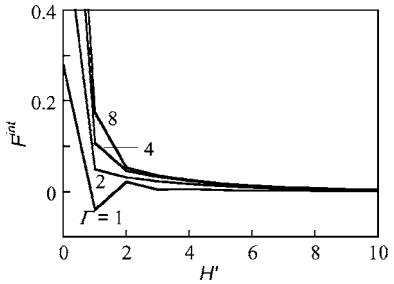

FIG. 7. Free energy of interaction in units of $k_BT/2l^2$ as a function of the separation H' in units l between the surfaces in semilogarithmic coordinates in the case of restricted equilibrium for $N=100$, $\chi=1.5$, and $\chi_S=-3$. The amount of polymer that is restricted is varied as indicated. Note that the distance H' is modified according to the restricted amount. For $\Gamma=1$ there is effectively very little restricted amount compared to the full equilibrium case where $\varphi(1) \approx 0.8$; however, the distance H is shifted by one unit.

cases when the restricted amount is varied. Inspection of Fig. 7 shows that indeed the curves very quickly become completely repulsive. Restricting just a few molecules to the surface is sufficient to mask the oscillations. More specifically when $\Gamma \approx 1$ on each of the surfaces, i.e., when the total adsorbed amount is $\Gamma \approx 2$ there is a shallow repulsion for $H' > 1$ and a steep repulsion for $H' < 1$. Such an intermediate case must be expected when a polymer melt with very small (mobile) polymer chains is compressed.

At this point it is interesting to speculate how to link the results as obtained by the partial equilibium SCF analysis to the dynamic interaction curves found in experiments. Obiously in experimental conditions, the time scale of approach and retraction will have an influence on the measured forces. The slower an experiment is performed, the more chains can freely exchange with the bulk. Qualitatively, one should expect a systematic change from the full equilibrium, via partial restricted cases (cf. Fig. 7), to the restricted equilibrium case, when the time scale of the experiment is decreased. How this mapping must be done quantitatively, remains an interesting problem to be solved.

V. CONCLUSIONS

We have developed a generalized restricted equilibrium ansatz for polymers in confined spaces applicable for semidilute and concentrated polymer solutions as well as polymer melts. Especially when the interfacial chains are translationally restricted, we predict short-range repulsive interaction caused by the fact that the interfacial chains are squeezed. The interaction curves typically have two exponentially decaying regimes. At very short distances the polymer volume fraction in the gap is significantly increased as compared to that of the bulk polymer melt, which leads to a steep repulsive force. The characteristic decay length is $3l-5l$. In practice, a system is likely to freeze into a glassy state. At larger distances (and thus lesser confinement), the force decays on the length scale of the size of the chains R_g. Here, the interfacial chains are compressed and, simultaneously, the free chains are pushed out of the gap. As the overall polymer density remains approximately the same as in the bulk, the interaction force remains relatively low. However, the forces are still large enough so that they can easily be picked up in a force experiment. The interaction curves, both in full as well as restricted equilibrium, do not depend much on the wetting characteristics of the system (i.e., they do not depend much on the adsorption energy). However, the applicability of the restricted equilibrium rests on the separation of time scales of lateral mobility between bulk chains and interfacial chains. This separation of time scales may, in part, be determined by the wetting characteristics.

[1] P. G. de Gennes, Acad. Sci., Paris, C. R. **305**, 1181 (1987).
[2] D. Ausserré, J. Phys. (Paris) **50**, 3021 (1989).
[3] G. ten Brinke, D. Ausserré, and G. Hadziioannou, J. Chem. Phys. **89**, 4374 (1988).
[4] R. Dickmann and C. K. Hall, J. Chem. Phys. **89**, 3168 (1988).
[5] P. G. de Gennes, Macromolecules **15**, 492 (1982).
[6] J. M. H. M. Scheutjens and G. J. Fleer, Macromolecules **18**, 1882 (1985). J. Colloid Interface Sci. **111**, 504 (1986).
[7] J. M. H. M. Scheutjens, G. J. Fleer, and M. A. Cohen Stuart, Colloids Surf. **21**, 285 (1986).
[8] A. N. Semenov, J. Bonnet-Avalos, A. Johner, and J.-F. Joanny, Macromolecules **29**, 2179 (1996).
[9] A. Johner, J. Bonnet-Avalos, C. C. van der Linden, A. N. Semenov, and J.-F. Joanny, Macromolecules **29**, 3629 (1996).
[10] E. F. Casassa, Polym. Lett. **5**, 7739 (1967).
[11] G. J. Fleer and F. A. M. Leermakers, in *Coagulation and Flocculation*, 2nd ed. (Surfacant Science Series 126), edited by H. Schechemesser and B Dobiáš (CRC, Boca Raton, 2005), Ch. 6, pp. 349–4563.
[12] W. K. Wijting, W. Knoben, N. A. M. Besseling, F. A. M. Leermakers, and M. A. Cohen Stuart, Phys. Chem. Chem. Phys. **6**, 4432 (2005).
[13] S. F. Edwards, Proc. Phys. Soc. London **85**, 613 (1965).
[14] P. G. De Gennes, *Scaling Concepts in Polymer Physics* (Cornell Univ. Press, Ithaca, NY, 1979).
[15] R. G. Horn, S. J. Hirz, G. Hadziioannou, C. W. Frank, and J. M. Catala, J. Chem. Phys. **90**, 6767 (1989).
[16] J. van Alsten and S. Granick, Macromolecules **23**, 4856 (1990).
[17] J. P. Montfort and G. Hadziioannou, J. Chem. Phys. **88**, 7187 (1988).
[18] S. Hirz, A. Subbotin, C. Frank, and G. Hadziioannou, Macromolecules **29**, 3970 (1996).
[19] M. Ruths and S. Granick, J. Phys. Chem. B **103**, 8711 (1999).
[20] J. N. Israelachvili and S. J. Kott, J. Phys. Chem. **88**, 7162 (1988).
[21] J. Luengo, F. J. Schmitt, R. Hill, and J. Israelachvili, Macromolecules **30**, 2482 (1997).
[22] J. M. Georges, S. Millot, J. L. Loubet, and A. Tonck, J. Chem. Phys. **98**, 7345 (1993).
[23] H. W. Hu and S. Granick, Science **258**, 1339 (1992).
[24] J. Peanasky, L. L. Cai, S. Granick, and C. R. Kessel, Langmuir **10**, 3874 (1994).
[25] R. G. Horn and J. N. Israelachvili, Macromolecules **21**, 2836 (1988).
[26] G. Sun, M. Kappl, and H.-J. Butt, Colloids Surf., A **250**, 203 (2004).
[27] G. Sun, M. Kappl, T. Pakula, K. Kremer, and H.-J. Butt, Langmuir **20**, 8030 (2004).
[28] G. Sun and H.-J. Butt, Macromolecules **37**, 6086 (2004).
[29] J. Klein, Nature (London) **288**, 248 (1980).
[30] J. N. Israelachvili, M. Tirrell, J. Klein, and Y. Almog, Macromolecules **17**, 204 (1984).
[31] Y. Almong and J. Klein, J. Colloid Interface Sci. **106**, 548 (1985).
[32] P. J. Flory, *Principles of Polymer Chemistry* (Cornell University Press, Ithaca, NY 1953).
[33] J. M. H. M. Scheutjens and G. J. Fleer, J. Phys. Chem. **83**,

1619 (1979).
[34] J. M. H. M. Scheutjens and G. J. Fleer, J. Phys. Chem. **84**, 178 (1980).
[35] G. J. Fleer, M. A. Cohen Stuart, J. M. H. M. Scheutjens, T. Cosgrove, and B. Vincent, *Polymers at Interfaces* (Chapman and Hall, London 1993).
[36] M. Schick, in *Liquids at Interfaces*, edited by J. Charvalin, J. F. Joanny, and J. Zinn-Justin (Les Houches, Amsterdam, 1988).
[37] J. M. H. M. Scheutjens and G. J. Fleer, *The Effect of Polymers on Dispersion Properties*, edited by Th. F. Tadros (Academic Press, London, 1982), p. 145.
[38] J. van Male, Ph.D. thesis Wageningen University, 2003 (unpublished).
[39] S. A. Safran, *Statistical thermodynamics of surfaces, interfaces and membranes* (Addison-Wesley, Reading, MA, 1994).
[40] F. A. M. Leermakers, J. H. Maas, and M. A. Cohen Stuart, Phys. Rev. E **66**, 051801 (2002).